Propeller and Kaplan Turbines

Propeller and Kaplan turbines are axial flow machines in which the flow through the runner is predominantly axial. A typical Kaplan turbine is shown in figure 1. The primary difference between the two is that the runner blades in a propeller turbine are fixed while the runner blades of a Kaplan turbine have an adjustable inclination.

Further examination of the fluid mechanics of these axial flow turbines requires definition of a thin cylindrical element of the flow through the runner at one particular radial location, r. Unwrapping that element it becomes a linear cascade with an infinite array of identical blades as shown in figure 2.

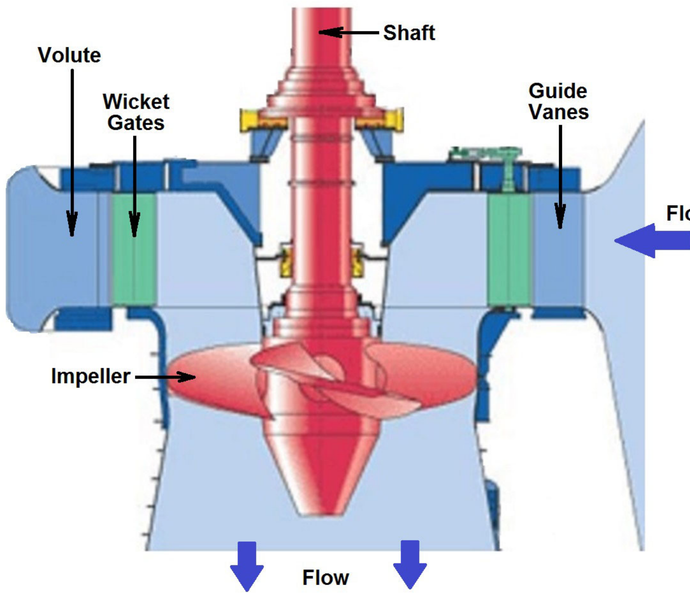

Figure 1: Schematic of a Kaplan turbine.

The flow through this linear cascade (and, by extension and integration, through the turbine impeller as a whole) can be analyzed in a manner parallel to that used for an axial flow pump in section (Mbcb). Here we provide just an outline of that approach using the control volume indicated in figure 2. Applying the momentum theorem to this control volume, the forces, F_x and F_y, imposed by the fluid on each blade (per unit depth normal to the sketch), are given by

$$F_x = (p_1 - p_2)h \quad \text{(Mdf1)}$$

$$F_y = \rho h v_m (w_1 \cos\beta_1 - w_2 \cos\beta_2) \quad \text{(Mdf2)}$$

where, as a result of continuity, $v_{m1} = v_{m2} = v_m$. To proceed, we define the vector mean of the relative velocities, w_1 and w_2, as having a magnitude w_M and a direction β_M, where by simple geometry

$$\cot\beta_M = \frac{1}{2}(\cot\beta_1 + \cot\beta_2) \quad \text{(Mdf3)}$$

$$w_M = v_m \big/ \sin\beta_M \quad \text{(Mdf4)}$$

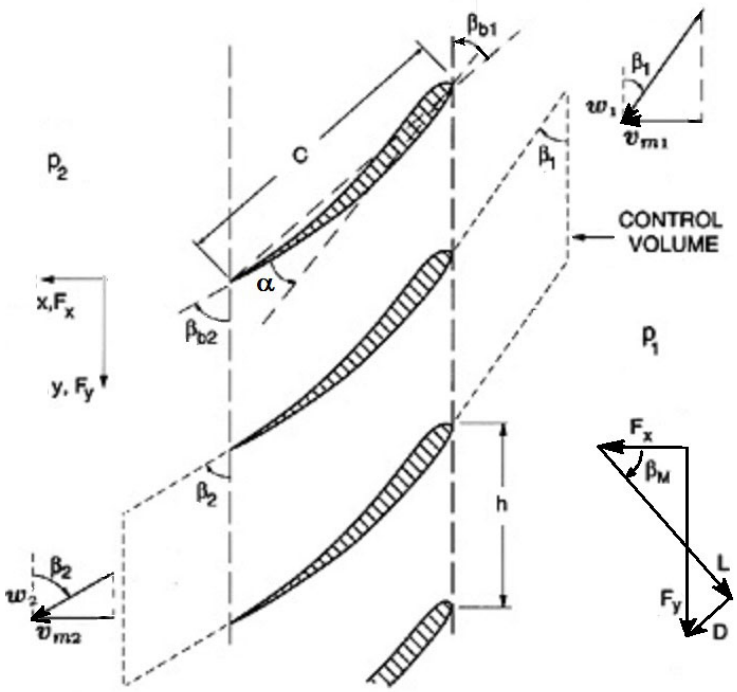

Figure 2: Schematic of a linear cascade showing the blade geometry, the periodic control volume and the definition of the lift, L, and drag, D, forces on a runner blade.

It is conventional and appropriate (as discussed below) to define the lift, L, and the drag, D, components of the total force on a blade, $(F_x^2 + F_y^2)^{\frac{1}{2}}$, as the components normal and tangential to the vector mean velocity, w_M. More specifically, as shown in figure 2,

$$L = -F_x \cos\beta_M + F_y \sin\beta_M \quad \text{(Mdf5)}$$

$$D = F_x \sin\beta_M + F_y \cos\beta_M \quad \text{(Mdf6)}$$

where L and D are forces per unit depth normal to the sketch. Non-dimensional lift and drag coefficients are defined as

$$C_L = L/\frac{1}{2}\rho w_M^2 c \quad ; \quad C_D = D/\frac{1}{2}\rho w_M^2 c \quad \text{(Mdf7)}$$

Estimates of C_D and C_L then permit evaluation of the total head loss in the runner and therefore the hydraulic performance of the runner. This will lead to a relation for the total head drop through the impeller as a function of the flow rate.

To continue we resume the fluid mechanical analysis begun in section (Mdi) by observing that we could modify the relation (Mdi1) to include viscous losses by writing that

$$p_1 - p_2 = \Delta p_L^T - \frac{\rho}{2}\left(w_1^2 - w_2^2\right) \quad \text{(Mdf8)}$$

where Δp_L^T denotes the total pressure loss in the flow through the runner caused by viscous effects. In frictionless flow, $\Delta p_L^T = 0$, and the relation (Mdf8) becomes the Bernoulli equation in rotating coordinates (equation (Mdi1) and (Mdi2)) with $r_1 = r_2$ as is appropriate here. A dimensionless loss coefficient, f, will be defined as

$$f = \Delta p_L^T/\rho w_M^2 \quad \text{(Mdf9)}$$

Equations (Mdf1) through (Mdf9) can be manipulated to obtain expressions for the lift and drag coefficients as follows

$$C_D \;=\; 2f\sin\beta_M/s \tag{Mdf10}$$

$$C_L = \frac{2}{s}\left[-\frac{\psi}{\phi}\sin\beta_M + \frac{f(\phi-\cos\beta_M\sin\beta_M)}{\sin\beta_M}\right] \tag{Mdf11}$$

where $s = c/h$ is the solidity, ψ is the head coefficient, $(p_1^T - p_2^T)/\rho\Omega^2R^2$, and ϕ is the flow coefficient, $v_m/\Omega R$.

It also follows from the above relations that the head coefficient, ψ, is given by

$$\psi \;=\; \phi\,(\cot\beta_2 - \cot\beta_1) + \frac{f\phi^2}{\sin^2\beta_M} \tag{Mdf12}$$

When there is no inlet swirl or prerotation so that $\tan\beta_1 = \phi$, equation (Mdf12) becomes

$$\psi = -1 + \phi\cot\beta_2 \;\; + f\left[\phi^2 + \frac{1}{4}\left(1+\phi\cot\beta_2\right)^2\right] \tag{Mdf13}$$

In frictionless flow, when the discharge is parallel with the blades ($\beta_2 = \beta_{b2}$), this has the form of the characteristic equation (Mdi8).

Note also that the use of the relation (Mdf13) allows us to write the expression (Mdf11) for the lift coefficient as

$$C_L = \frac{2}{s}\left[2\sin\beta_M(\cot\beta_1 - \cot\beta_M) - f\cos\beta_M\right] \tag{Mdf14}$$

Figure 3 presents examples of typical head/flow characteristics resulting from equation (Mdf13) for some chosen values of β_2 and the friction coefficient, f. It should be noted that, in any real turbomachine, f will not be constant but will vary substantially with the flow coefficient, ϕ, which determines the angle of incidence and other flow characteristics. Note that this typical family of performance curves essentially

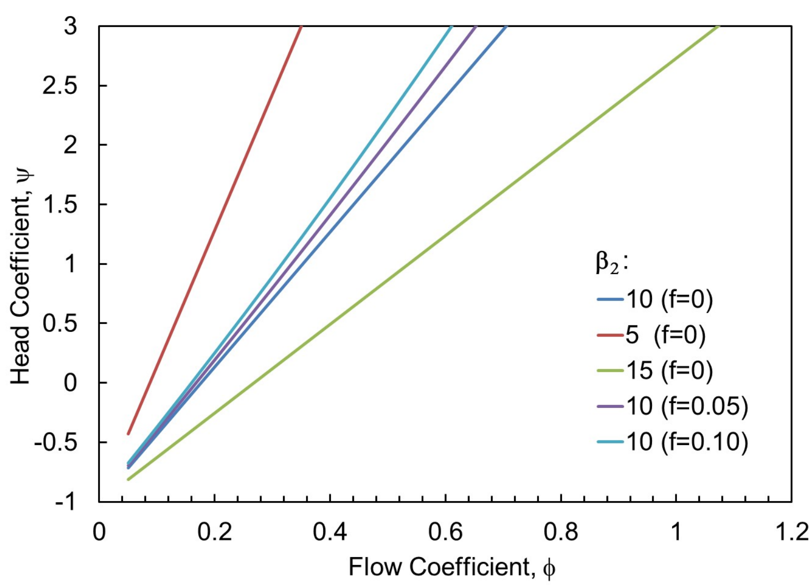

Figure 3: Calculated head/flow characteristics for some linear cascades.

mirrors the family of performance measurements presented in section (Mdj).

The observant reader will have noted that all of the preceding equations of this section involve only the inclinations of the flow and *not* of the blades, which have existed only as ill-defined objects that achieve the turning of the flow. In order to progress further, it is necessary to obtain a detailed solution of the flow, one result of which will be the connection between the flow angles (β_M, β_2) and the geometry of the blades, including the blade angles (β_b, β_{b1}, β_{b2}). A large literature exists describing methods for the solutions of these flows, but such detail is beyond the scope of this text.

To begin with, however, one can obtain some useful insights by employing our basic knowledge and understanding of lift and drag coefficients obtained from tests, both those on single blades (airfoils, hydrofoils) and those on cascades of blades. One such observation is that the lift coefficient, C_L, is proportional to the sine of the angle of attack, where the angle of attack is defined as the angle between the mean flow direction, β_M, and a mean blade angle, β_{bM}. Thus

$$C_L = m_L \sin(\beta_{bM} - \beta_M) \qquad \text{(Mdf15)}$$

where m_L is a constant, a property of the blade or cascade geometry.

In the case of frictionless flow ($f = 0$), the expression (Mdf15) may be substituted into equation (Mdf14), resulting in an expression for β_M. When this is used with equation (Mdf13), the following head/flow characteristic results:

$$\psi = \frac{2m_L s \sin\beta_{bM}}{4 + m_L s \sin\beta_{bM}} \left[\phi \left(\cot\beta_{bM} + \frac{v_{\theta 1}}{v_{m1}} \right) - 1 \right] \qquad \text{(Mdf16)}$$

Note that, unlike equation (Mdf13), the head/flow characteristic of equation (Mdf16) is given in terms of m_L and practical quantities, such as the blade angle, β_{bM}, and the inlet swirl or prerotation, $v_{\theta 1}/v_{m1}$.

It is also useful to consider the drag coefficient, C_D, for it clearly defines f and the viscous losses. Instead of being linear with angle of attack, C_D will be an even function so an appropriate empirical result corresponding to equation (Mdf15) would be

$$C_D = C_{D0} + m_D \sin^2(\beta_{bM} - \beta_M) \qquad \text{(Mdf18)}$$

where C_{D0} and m_D are constants. Using typical values of C_{D0} and m_D (for example, $C_{D0} = 0.02$ and $m_D = 0 - 2$) equation (Mdf18) allows estimates of C_D and hence of f using equation (Mdf10). These values of f are ordinarily much larger at small flow coefficients and result in much larger head coefficients at the low flows as exemplified by Figure 1 of section (Mdj).